

Static Equilibrium of the Triangular Running Skyline System: A Three Dimensionally Movable Cable System

Y. Suzuki¹
Kyoto University
Kyoto, Japan²

E.S. Miyata
S.C. Iverson
University of Washington
Seattle, USA

ABSTRACT

The static equilibrium of the Triangular Running Skyline (TRS) system was tested using a reduced scale model to see if and to what degree the carriage location and line tensions at the spars differed from the theoretically predicted ones. TRS is one of the promising environmentally sound methods for accessing the forest. The model has a span of three meters so that all conditions can be dealt with on a laboratory basis. In this test, line lengths of this model system were designed to have unstretched lengths derived from the theory of elastic catenary, to have the carriage set at a designated position. Then, the measured positions of the carriage and line tensions were compared with those derived from the theory. The results proved that the horizontal positioning error of the carriage is smaller than its vertical positioning error and that the carriage tends to be lower than its theoretical value. The greater theoretical line tension causes the error in line tension to be larger and the line tension tends to be lower than the theoretical value. In order to obtain more accurate positioning of the carriage, it is necessary to take loosening of lines, guy lines of spars, etc. into account.

Keywords: *Triangular Running Skyline system, cable system, scale model, position control, static equilibrium.*

¹The authors are, respectively, Assistant Professor of Forest Engineering, Principal Research Scientist of Industrial Engineering, and Associate Professor of Industrial Engineering.

²Current address: Kochi University, Kochi, Japan.

INTRODUCTION

There is a need for the introduction of an environmentally sound method for the logging of forests and the making of scientific observations there. The Triangular Running Skyline (TRS) system is a promising method to obtain this goal. The system has one head spar and two tail spars to enable the carriage to move around in a pertinent triangular area (Figure 1); the carriage of an ordinal cable system moves only between the single tail spar and the head spar. One study developed an actual TRS system and ascertained the effect of the system by field operations [7]. In their TRS system, the carriage positioning was manually controlled on the assumption that a total line length would be constant. However, as a result of the field operations, it has been proved that a more accurate control of carriage position is necessary to prevent damage to forests (Kanzaki, personal communication). Meeting this goal would necessitate the discovery of the detailed static equilibrium of the TRS system, yet there has been no such study available to date.

The purpose of the present study is to predict in an actual TRS system how much difference exists in carriage positions from a designated point. We assumed that a carriage position is not controlled by the line tension, but by the line lengths [6], saying that when the carriage position is controlled by the line tensions, the positioning error of the carriage would not be reduced unless an appropriate mechanism is adopted in the TRS system to accurately control the line tension.

MATERIALS AND METHODS

Overview

We designed a TRS model that was reduced in length to a scale of 1/100 of a desired real system so that all the necessary conditions could be dealt with on a laboratory basis. However, the ratio of a load weight to a line weight per unit length (unit line weight) was greater than the scale ratio of the model. The essential role for any cable system is to move a carriage with or without a load to a designated point while keeping line tensions in a safe range. The model designed is analogous to the TRS system controlled by line lengths. The model consists of a steel framework, pulleys, three sets of tension devices, wire ropes, and a weight. The line lengths are calculated to locate the carriage at the designated point that keeps the line tensions less than the preset

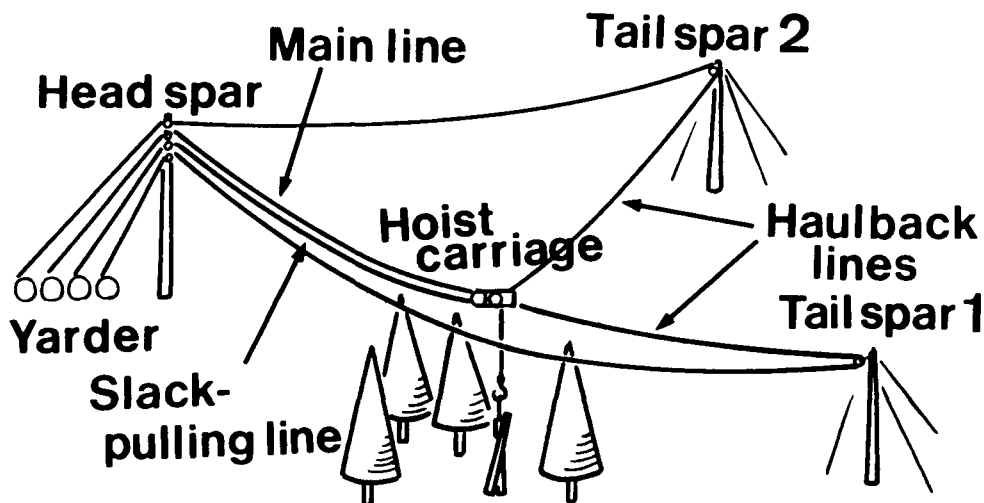


Figure 1. Triangular Running Skyline system.

maximum value. When setting the line lengths, both the position of the load point and the line tensions of the model can be observed. Differences between the theoretical and experimental configurations suggest that the directional positioning errors of the carriage may possibly occur in the real system.

We have derived the theoretical solutions using the methods proposed by others [13]. Those methods are based on an application of the theory of elastic catenary [2, 3, 9, 10, 11, 12] to the previous theoretical studies of the TRS system [4, 5], with consideration for cable stretching. In this study, the main and slack pulling lines of the TRS system are treated as one line for simplicity [4, 5, 13].

Equipment

The framework of the scale model is a triangular-prism truss approximately 1.5 m high and 3.0 m long on each side (Figures 2 and 3). The framework used as the top and side members of the model consists of L-shaped steel beams whose cross-section is 2.54 cm wide on each side. The framework used as the bottom members consists of L-shaped steel beams whose cross-section is 5.08 cm wide on each side. All of these steel beams are 3.18 mm thick. The pulley attached to the top end of each vertical member plays the role of a block on the spar (Figure 4). Assuming the frame to have an ideal truss, the

maximum displacement of the top end is estimated to be less than $0.15 \cdot 10^{-3}$ mm/N in accordance with the principle of virtual work [1], which also provides steel properties]. The effect of the frame displacement is negligible because the forces applied to the top ends were in the order of 10 N or less throughout all our tests.

We measured the line tensions using our own developed tension generating devices that can roughly double the line tension and can transmit the line tension to a load cell horizontally placed (Figure 5). Each load cell has a capacity of 981 N. The calibration accuracy certified by the manufacturer indicates that an error in calibration accuracy due to temperature fluctuation is $98.1 \cdot 10^{-3}$ N (98.1 mN). Therefore, it is expected that the possible error due to temperature fluctuation is 49.1 mN. The A/D (analog-to-digital) converter used in this model converts the output from the load cell to numeric digits. When the calibration is done properly, the converter displays an unmodified line tension at a resolution of 9.81 mN (1 gf). After a preliminary test was executed, we found that the friction between the pulley and the wire rope is negligible (μ_s , static coefficient of friction < 0.005), while the response from the tension generating devices is not linear. We could not specify the causes such as the hysteresis of the load cell, the friction between the load cell and the tension generating device, the geometric nonlinearity of the tension generating device, etc.

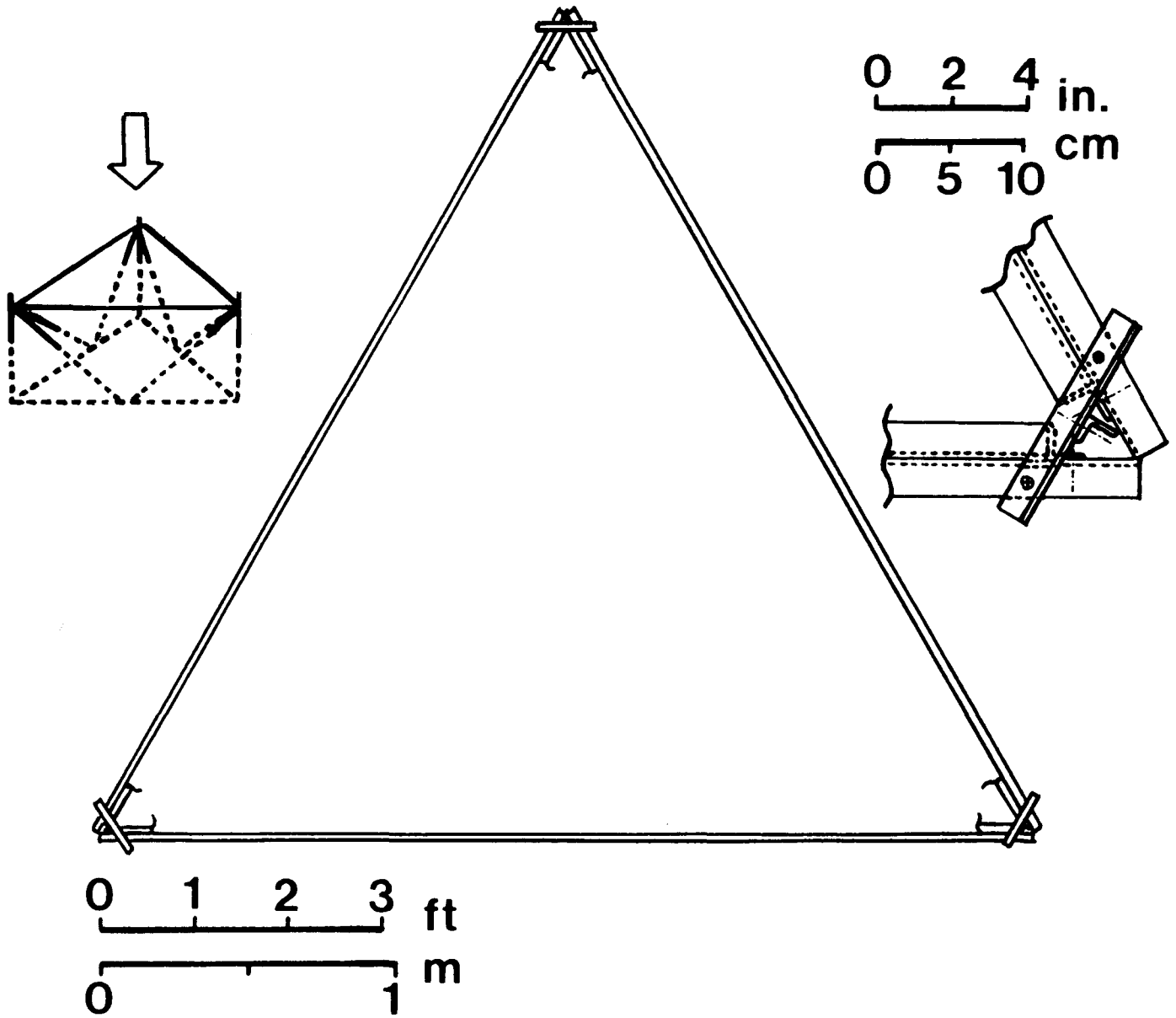


Figure 2. Truss framework of the scale model: Top view.

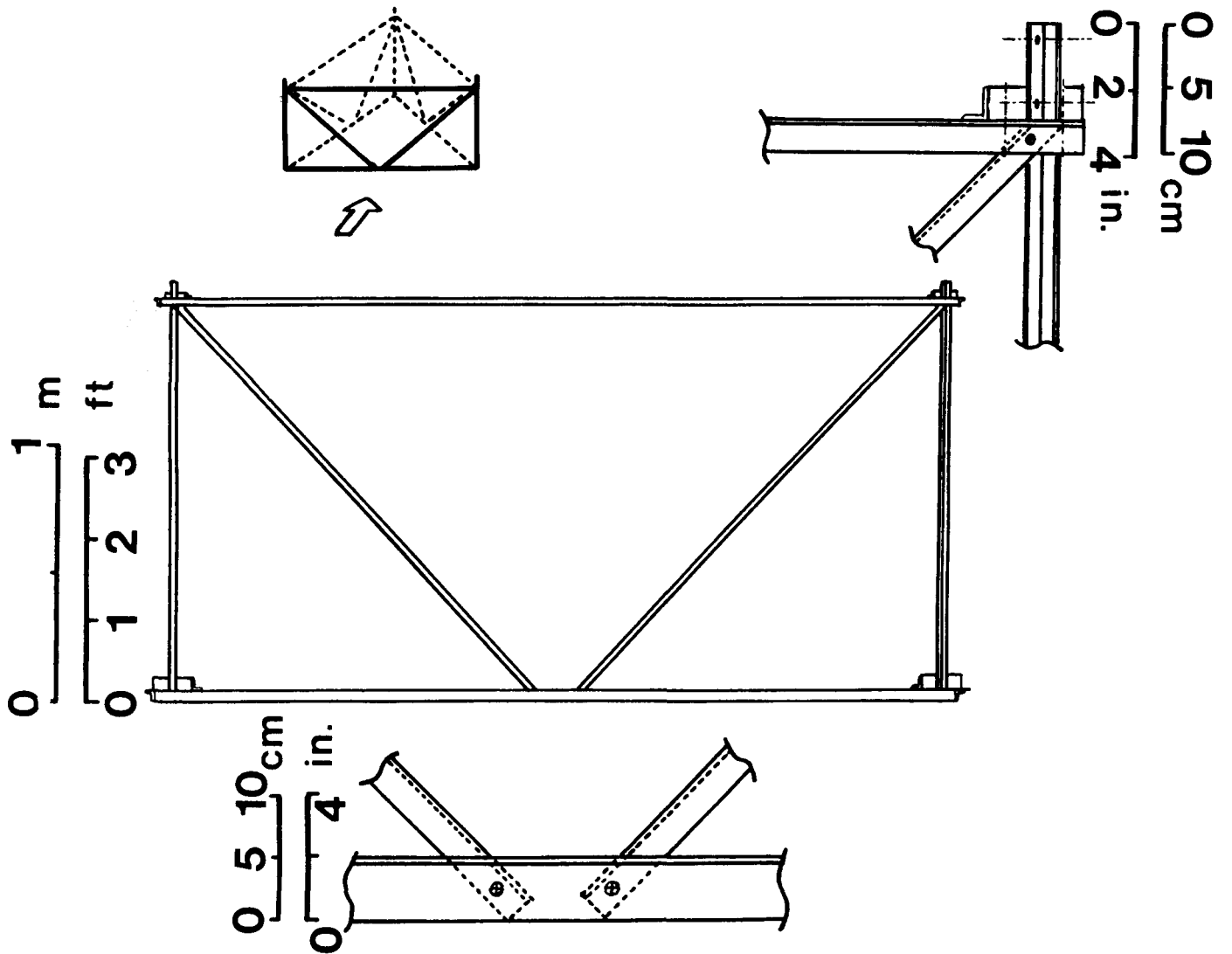


Figure 3. Truss framework of the scale model: Side view.

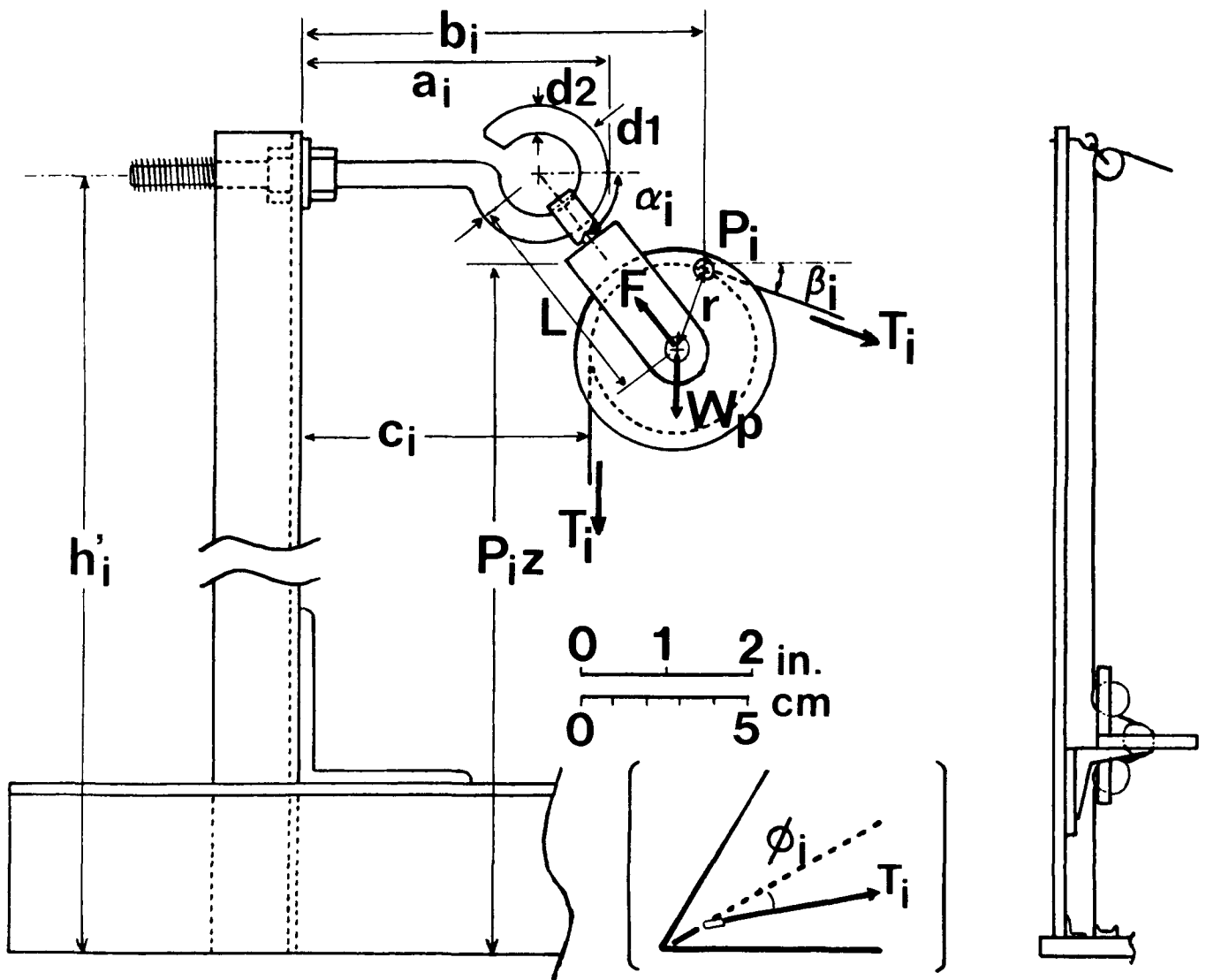


Figure 4. Pulley and vertical member of the framework. Inset: Top view of a corner of the framework.

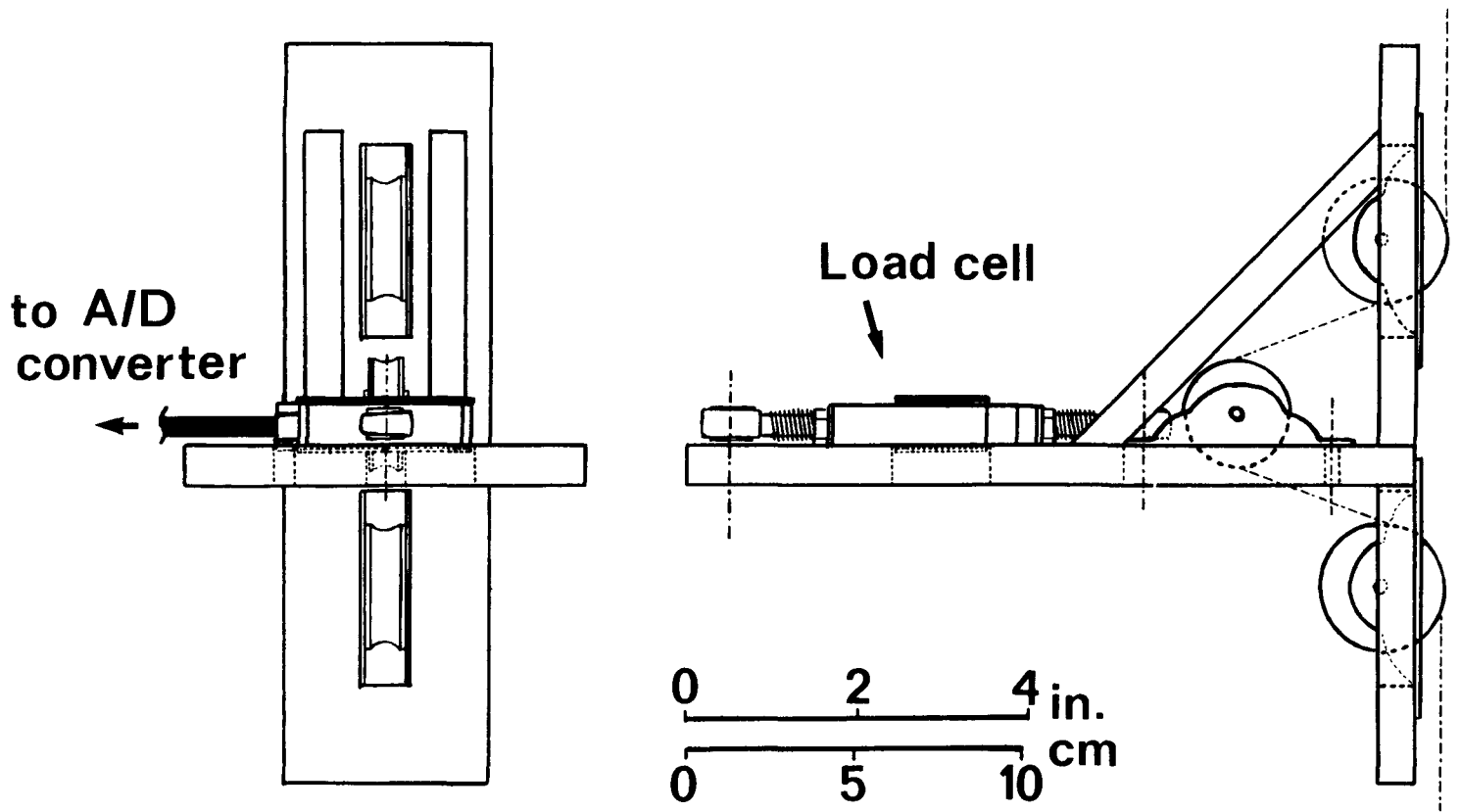


Figure 5. Tension generating device.

Therefore, we tested each tension generating device and derived correcting functions by means of regression (2nd order; each tension generating device was tested 35 times; $r^2 > 0.995$) to obtain an accurate line tension.

There were a few possibilities of selecting wire rope type to avoid the effect of bending stiffness. We selected two types of wire rope (Table 1). One type of wire rope (FF054) has a diameter of 0.54 mm, and the other (FF072) 0.72 mm. Both types of wire rope are made of stainless steel, and they have a structure of 7×7 (the products of Nippon Miniature Rope). We measured the mass of unit line length and modulus of elasticity (E) of each type of wire rope. Their moduli of elasticity were obtained from tensile tests. Each wire rope was tested for modulus of elasticity 35 times applying the maximum load of 26.3152 N. In the tensile tests, each loading took about ten minutes, which is almost the same duration taken for each static equilibrium test. While observing some non-linear response, the modulus of elasticity was estimated by means of linear regression ($r^2 = 0.912$ for FF054 and 0.948 for FF072).

The load used as weight is a small hook. Three wire ropes are connected to the weight via a ring. A total mass of the ring and weight (W) is 1.7110 N. During the experiment, we observed the permanent bending that occurred at a knot at the ring and some intermediate points on wire ropes, especially on FF054. Although the occurrence of permanent bending is inevitable, it might be a source of the positioning errors of the weight.

Table 1. Characteristics of the wire ropes.

Material Structure	Stainless steel 7×7	
	FF054	FF072
Type		
Diameter (mm)	0.54	0.72
Breaking strength (N)	2.55	4.79
Section, A (mm ²)	0.13854	0.24630
Unit mass (g/cm)	0.01243	0.02066
Modulus of elasticity, E (GPa)	35.93	29.29

Notes: Unit mass and modulus of elasticity are obtained from the test. The other data are obtained from the manufacturer.

Measurement

A procedure to obtain a set of observations consists of a number of steps such as setting the line lengths, rigging up the lines with a weight on the framework, making accurately marked points of the lines coincide with the pulleys, fastening line ends to the framework, measuring the height of the load point, recording the line tensions, measuring the position of the load point on a plane, and measuring the heights of anchor points. We divided the experiment into three groups. Before executing the measurement of each group, we calibrated the A/D converters with maximum capacity of 19.0682 N. We measured all of the lengths, that is, the unstretched line lengths, the height and plane position of the weight, and the height of anchor points up to 0.1 mm to ensure an accuracy of 1 mm. The following describes the procedure.

First, before rigging up the lines, each line length from the knot was measured to mark a theoretically obtained length using a piece of stick tape. Then, the lines were rigged up to hang a load at a designated point. The ends of lines are tightened to a bar at the bottom of the framework (see the right-hand side of Figure 4). For FF054, each line was wrapped around the bar two or more times and fastened to it with a pair of clips. For FF072, a vise-grip, a device for holding a matter firmly using a lever, fastens the wire rope without wrapping to prevent the occurrence of permanent bending. Rubber strips wrapped around and stuck over each bar prevent the lines from slipping. The direction of the marked point on the line must coincide with a tangent on the pulley (P_i of Figure 4).

When the entire system becomes stable after rigging up the lines, a steel ruler is used to measure the height of a load point. Then the line tensions are recorded, which are corrected by the functions for the devices. Next, a chain weighing 1.1085 N is hung down on a hook to mark a plane projection of the load point on the floor. This causes a slight movement of the load point. Thus, the theoretical plane positions of the carriage are recalculated with $W = 1.7110 + 1.1085 = 2.8195$ N. By measuring at least two lengths from the established points on the floor to the projected point, the horizontal coordinates of the load point are obtained. We used three points located right under the pulleys as the established points. Those include one redundant point which helps to detect and correct measuring errors. Lastly, distances between the ground and tangen-

tial points on a pulley are measured, which are the heights of anchor points (Pz).

Theoretical Values

We derived theoretical values from the two methods proposed in [13], named Problems I-a and III in the reference. When the designated planar coordinates of the carriage (Pd_x, Pd_y), and the maximum line tension T_{max} are given, the method of Problem I-a derives the height of carriage Pd_z , stretched line tensions s_i (i denotes line number), and line tensions at the anchor points T_i . Given parameters for the method of Problem I-a are the coordinates of three spars P_i , line properties (modulus of elasticity E_i , unit weight ω_i , and section area A_i), and weight of the load W . The method of Problem III derives the coordinates of carriage P_i, s_i , and T_i from $P_i, E_i, \omega_i, A_i, W$, and unstretched line lengths Lo_i .

In an actual TRS system, the movement of anchor points is negligible. However, the pulleys of the model are large compared to the scale ratio as shown in Figure 4. The movement depends on the vector of line tensions. To take the movement into account, the following iterative procedure must be adopted.

First, we explain the movement of the pulleys. Let (ϕ_i be the angle included between horizontal i_{th} line direction and the center line of the hook hanging the i_{th} pulley (see the inset of Figure 4). Let both α_i and β_i be the angle of the pulley and the angle of the line with respect to the level line, respectively. Then, angle α_i can be expressed as follows:

$$\alpha_i = \tan^{-1} \left[\left\{ \left(W_p / T_i + 1 \right) \sec \beta_i + \tan \beta_i \right\} \sec \phi_i \right] \quad (1)$$

where W_p is the weight of the pulley (0.4639 N). Here it is assumed that the pulley is kept vertical. With these angles and dimensions of the framework and the pulleys, position P_i of the i_{th} anchor point can be calculated.

The execution of the procedure is started by applying the method of Problem I-a [13]. First, when designated planar coordinates (Pd_x, Pd_y) and the maximum line tension T_{max} are given, $P_i^{(0)}$ (the initial P_i) is taken with respect to certain $\theta_i^{(0)}$ and $\beta_i^{(0)}$. (Superscripts denote iteration.) We used 0° and 10° , respectively. We also defined ($P_{ix}^{(0)}, P_{iy}^{(0)}$) as the origin, and took the x-axis in parallel to the frame (Figure 6). The method of Problem I-a gives $Pd^{(0)}$,

$s_i^{(0)}$, $T_i^{(0)}$, and $\beta_i^{(1)}$. Note that we used this $s_i^{(0)}$ for unstretched line length Lo_i , which hereafter is constant. Then, $\theta_i^{(1)}$ is calculated from $P_i^{(0)}$ and $P_d^{(0)}$. With angles $\theta_i^{(1)}$ and $\beta_i^{(1)}$, and dimensions of the framework, equation (1) provides $\alpha_i^{(1)}$ and then $P_i^{(1)}$. Because Lo_i, ω_i , and W are given as constants, the method of Problem III [13] derives $P_d^{(1)}, m_i^{(1)}, T_i^{(1)}$, etc. from $P_i^{(1)}$. Note that $\beta_i^{(2)}$ has been obtained, followed by $\theta_i^{(2)}$. These steps should be repeatedly executed until the average of $|P_i^{(k+1)} - P_i^{(k)}|$ reaches a value less than 10^{-3} cm. (The iteration was less than 10 with data from the present study.) Therefore, the final configuration of the static test can be obtained.

We designed the experiment to figure out factors causing positioning and tension errors. Here, the term "error" means the difference between the theoretical and experimental values. The errors are the horizontal (e_{xy}) and vertical (e_z) positioning error of the load point, and tension error (e_T). We also evaluated an error in anchor point heights (e_{pz}) to check the movement of pulleys was correctly estimated or not. The factors are the relative location of a load point (Factor A), maximum line tension (Factor B), repetition (Factor C), and type of wire rope (Factor D). For e_T and e_{pz} , Factor A cannot be applied because they are defined for each line. Instead, line length (Factor F) and line number (Factor G) are concerned with them.

We defined three levels for Factor A with respect to force equilibrium. The levels are the corner (A1), the edge (A2), and the center (A3). On the corner, a line tension at the nearest anchor point exceeds the other levels since the horizontal force on the corner at the load point is the largest. In the neighborhood of the edge, the line tension at the anchor point farthest from the edge is very small while the others balance with each other. Lastly, all the line tensions reach almost the same at the center. When maximum line tension is kept constant, T_i (magnitude of i_{th} line tension) is roughly in inverse proportion to planar distance between P_i and P_d . Each location contains six points. Figure 6 shows numbered positions of these 18 points. (A1: 1 to 6, A2: 7 to 12, A3: 13 to 18.)

Factor B has two levels, $2W$ and $4W$. Levels of Factor D are FF054 and FF072. In each configuration, three lines are of the same in type of wire rope. Therefore, there are $18 \times 2 \times 2 = 72$ configurations in total. We tested for each configuration twice (C1 and C2). Therefore, there are 144 observations for e_{xy} and e_z and 432 observations for e_T and e_{pz} .

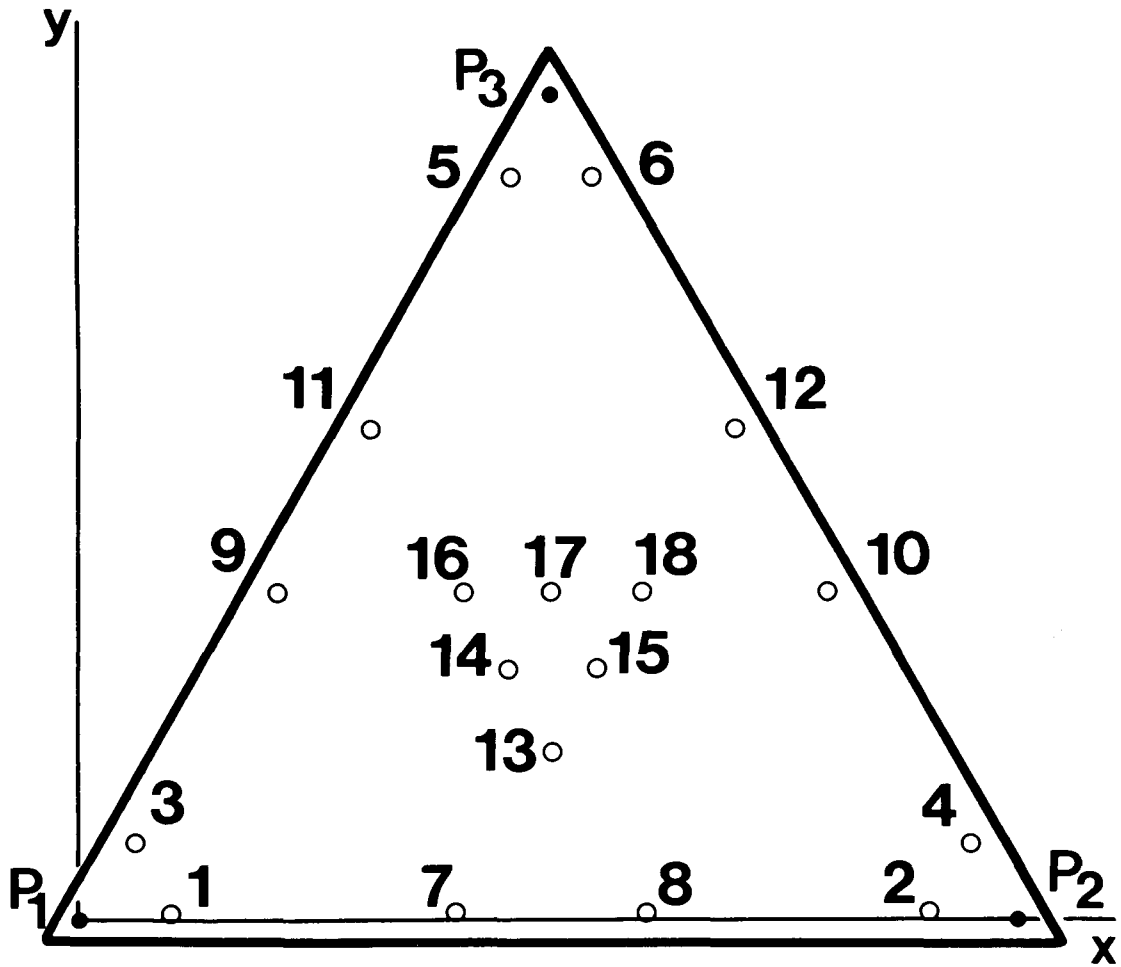


Figure 6. Location of tested points on a plane.

Table 2 lists the factors with their levels. Each level of Factor F, line length, contains the same number of observations in each level of the other factors so that the design of the experiment can be completed. That is, these factors are orthogonal to one another. It should be noted that Factor C, repetition, and Factor G, line number, represent experimental errors. The effect of the repetition (C) is assumed to involve the skill of an experimenter, and the effect of the line number (G) is assumed to involve the inequality of lines, pulleys, tension devices, etc.

RESULTS

Table 3 is the result of the Analysis of Variance (ANOVA) of e_{xy} in which the interactions between factors that were taken into consideration were limited to those between each two factors to avoid inappropriate complexity. We pooled the sum of squares (SS) of insignificant factors in the error factor (parenthesized "Error"). A contributing portion (indicates how much the factor contributes to the total SS (SS_T), and is defined by the following formula [14]:

$$P_j = (SS_j - DF_j \times MS_E) / SS_T \quad (2)$$

where subscript j denotes a factor concerned, DF the degree of the freedom of the factor, and MS_E the pooled mean square error.

Table 2. Definition of factors.

Factor	Symbol	Levels	1	2	3
Relative location	A	3	Corner	Edge	Center
Maximum tension	B	2	Low, 2W	High, 4W	
Repetition	C	2	1st	2nd	
Type of wire rope	D	2	FF054	FF072	
Line length	F	3	Short	Medium	Long
Line number	G	3	1	2	3

Table 3. ANOVA table of e_{xy} , the plane positioning error.

Source of Variance	Degree of Freedom	Sum of Squares	Mean Squares	F-value	p-value	p
A	2	0.28	0.141	0.84	43.3%	
B	1	0.05	0.053	0.31	57.6%	
C	1	0.97	0.972	5.80	1.7%	*
D	1	3.89	3.891	23.24	0.0%	**
A × B	2	0.23	0.117	0.70	50.0%	
A × C	2	0.18	0.091	0.54	58.4%	
A × D	2	0.12	0.059	0.35	70.3%	
B × C	1	0.36	0.355	2.12	14.8%	
B × D	1	0.30	0.303	1.81	18.1%	
C × D	1	0.88	0.879	5.25	2.4%	*
Error	129	21.60	0.167			
(Error)	140	23.12	0.165			81.8%
Total	143	28.86				100.0%

Notes: N = 144, Mean = 0.73 cm, ** = Significant at 1%, * = 5%.

Figure 7 depicts the effects of significant factors on e_{xy} , C and D with CxD. A horizontal line denotes a total mean of e_{xy} , which is less than 1 cm (0.73 cm). Each dot represents the average of e_{xy} for each level. Vertical lines represent Fisher's *protected* Least Significant Differences (LSD) at $p = 0.05$ [8]. Those LSD's are termed *protected* when the pooled mean square error, $MS_{E, \bar{y}}$ is used. We prefer the LSD rather than other statistic approaches for pairwise comparisons of levels (e.g., Duncan's multiple range test), because of its visual advantage. Among two factors and one interaction illustrated in the figure, only the type of wire rope (D) has levels which are clearly different from each other. That is, the horizontal positioning error of load point on level FF054 (D1) was apparently greater than that on FF072 (D2).

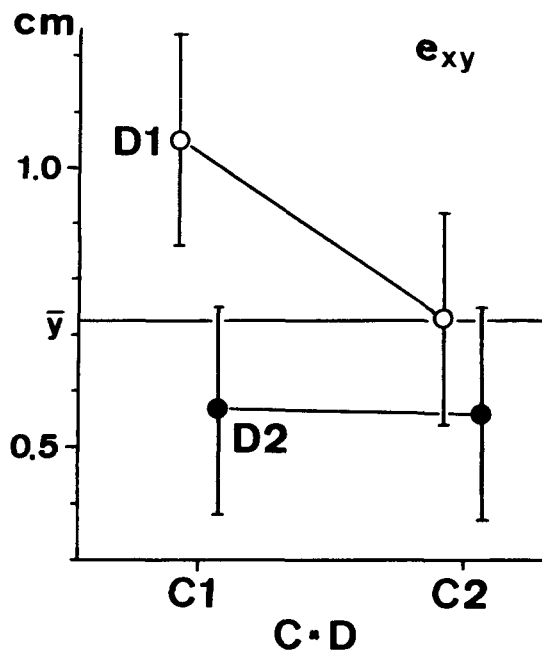


Figure 7. Effects of the repetition (C), the type of wire rope (D), and their interaction on e_{xy} the plane positioning error.

As stated in the section "Equipment", the permanent bending occurred on the wire ropes, especially for the thinner type (FF054). If the stretching force applied on the line is small, the permanent bending makes the stretched line length shorter than that with no permanent bending. When distance between the load point and the corresponding anchor point is large, the stretching force or tension

on the line is small. Therefore, the effect of permanent bending is greater when the length of the line concerned is longer.

To inspect the effect of permanent bending of wire ropes on the direction of e_{xy} , an error e_{lmax} is defined as follows (Figure 8). Let l_i and l'_i be the theoretical and observed planar distances between i_{th} anchor point P_i and the load point P_d' , respectively. Note that l'_i is calculated from the observed load point and the theoretical i_{th} anchor point. Letting l'_{max} be the largest l'_i among the three l'_i 's, e_{lmax} is defined by the following formula:

$$e_{lmax} = l'_{max} - l_{max} \tag{3a}$$

where

$$l_{max} = \max(l_i \mid i = 1 \text{ to } 3) \tag{3b}$$

If e_{lmax} is negative, the observed plane load position is closer to P_i than the theoretically obtained plane load position. This means the effect of permanent bending on the line of l_{max} . To see the effect of permanent bending on the wire ropes, e_{lmax} was analyzed in the same manner as e_{xy} .

The average of e_{lmax} was very small (-0.01 cm). Factor D, the type of wire rope, was not significant on e_{lmax} . Significant factors are A, the relative location of the load point, and C, the repetition. At the edge (A2) of the relative location, e_{lmax} was negative

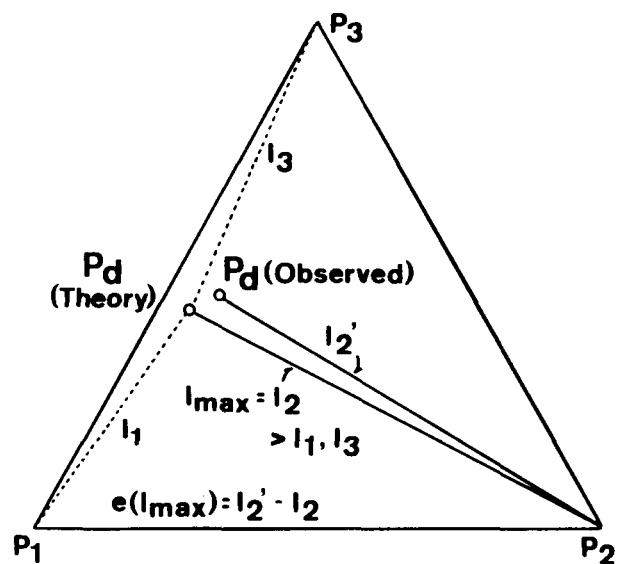


Figure 8. Definition of e_{lmax} .

(-0.28 cm) and positive (0.28 cm) at the corner (A1). e_{lmax} was nearly zero (-0.04 cm) at the center (A3). p of Factor A was 11.7 %. At the level of C1 (1st repetition), the average e_{lmax} was small negative (-0.14 cm) while small positive at C2 (0.11 cm). However, the difference is not apparent ($p = 3.3$ %). Considering that the average of e_{lmax} was much smaller than e_{xy} and that the type of wire rope (Factor D) was not significant, the effect of permanent bending on the wire ropes was negligible.

line tension (B) or the wire rope type (D) and the line length (F) tends to be smaller as the line length is longer. The reason is that inaccurate setting of line lengths affects the occurrence of tension error more when the line lengths are shorter. The factors of repetition (C), line number (G), and their interactions are significant, whereas their p 's are about two

Table 4. ANOVA table of e_z , the height positioning error.

Source of Variance	Degree of Freedom	Sum of Squares	Mean Squares	F-value	p-value		p
A	2	70.32	35.16	21.96	0.0%	**	14.9%
B	1	136.95	136.95	85.51	0.0%	**	30.1%
C	1	0.11	0.11	0.07	79.5%		
D	1	5.06	5.06	3.16	7.8%		
A × B	2	11.49	5.74	3.59	3.1%	*	1.8%
A × C	2	8.55	4.27	2.67	7.3%		
A × D	2	7.75	3.87	2.42	9.3%		
B × C	1	0.70	0.70	0.44	50.8%		
B × D	1	0.56	0.56	0.35	55.7%		
C × D	1	1.82	1.82	1.14	28.8%		
Error	129	206.59	1.60				
(Error)	138	231.14	1.67				53.2%
Total	143	449.90					100.0%

Notes: N = 144, Mean = - 3.18 cm, ** = Significant at 1%, * = 5%.

Table 4 is an ANOVA table of e_z . The mean (-3.18 cm) is a negative value greater than that of e_{xy} . Actually, almost all observed load points were lower than the theoretical height. Factors of relative location (A), maximum tension (B), and their interaction (A×B) are significant. Figure 9 shows the effects of those factors. The error is greater at both the edge (A2) and the center (A3) than that at the corner (A1). For the maximum tension, the error is greater at higher level (B2). Factor B, the maximum tension, has large p value (30.1%).

As shown in Table 5, the maximum tension is the strongest factor to the tension error, e_T . Figures 10 and 11 depict the effects of the maximum tension (B), the type of wire rope (D), and their interactions with the line lengths (F), respectively. When the maximum line tension is greater (B2) and the wire rope is thinner (D1), the mean of tension error e_T is negative. The interaction between the maximum

percent or less.

Finally, we reviewed the error of anchor point heights, e_{pz} . Although e_{pz} has fewer effects an actual system, it is important to mention it because anchor points are the basis of the theoretically obtained configurations in the present study. We measured no plane position of anchor points, because accurate measurement of them is difficult due to the arrangement of the framework. The mean error was a small negative value (- 0.12 cm). The factors that are significant and have large p were, in order of p , line length F (16.9%), line number G (6.1%), maximum line tension B (3.3%), and repetition C (3.2%). There were two significant interactive effects, C×D and D×G while their p 's were below 2%. When line length (F) was shorter, its effect was greater. The reason is, as mentioned in the tension error, that the effect of inaccurate line length is greater when the designed line length is shorter. Factor G, the line number, is assumed to involve inequality of pulleys and its peripherals. For the repetition (C), the error

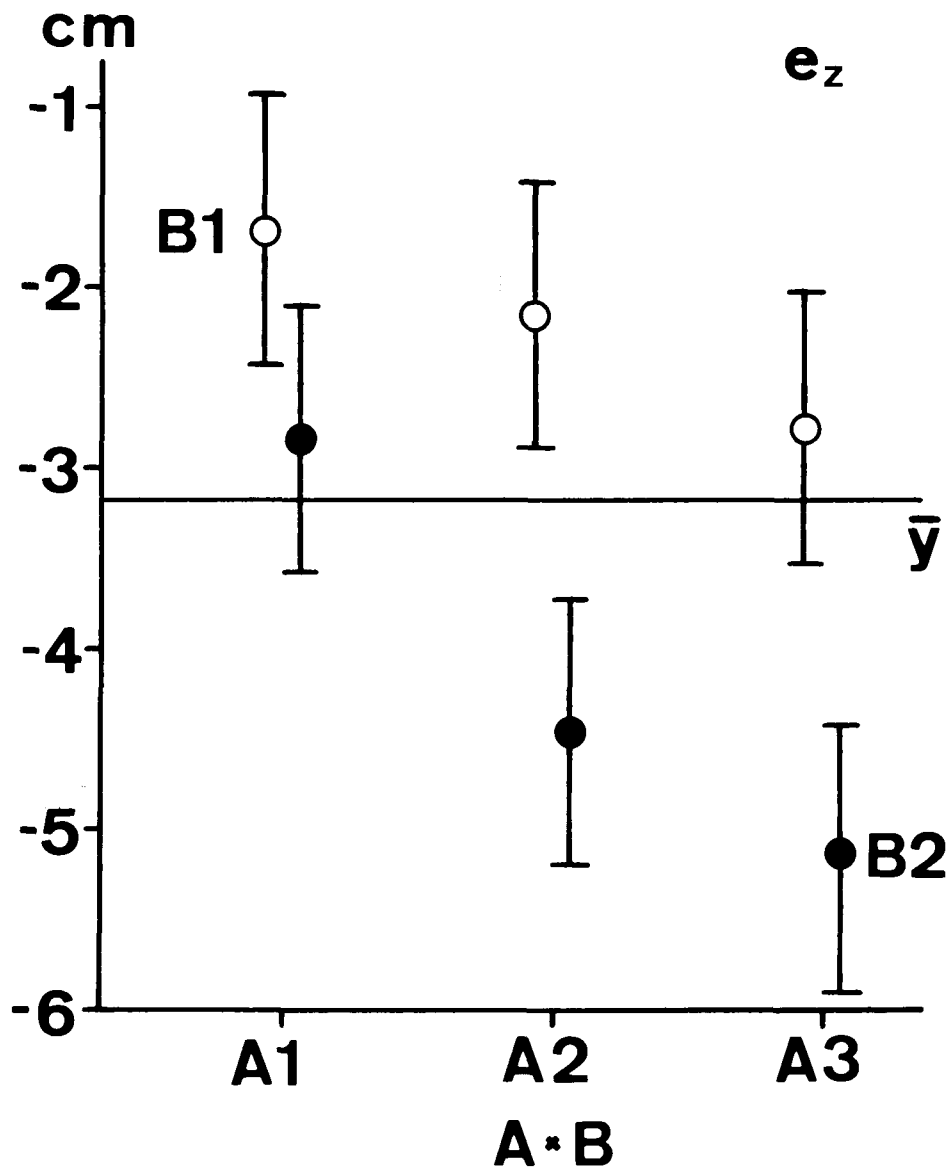


Figure 9. Effects of the relative location (A), the maximum line tension (B), and their interaction on e_z , the height error.

Table 5. ANOVA table of e_T , the tension error.

Source of Variance	Degree of Freedom	Sum of Squares	Mean Squares	F-value	p-value		<i>p</i>
B	1	46.45	46.45	255.44	0.0%	**	29.6%
C	1	1.79	1.79	9.85	0.2%	**	1.0%
D	1	12.87	12.87	70.78	0.0%	**	8.1%
F	2	0.50	0.25	1.37	25.5%		
G	2	3.04	1.52	8.35	0.0%	**	1.7%
B × C	1	0.06	0.06	0.32	57.3%		
B × D	1	0.56	0.56	3.10	7.9%		
B × F	2	6.18	3.09	16.99	0.0%	**	3.7%
B × G	2	2.93	1.46	8.05	0.0%	**	1.6%
C × D	1	0.02	0.02	0.12	72.7%		
C × F	2	0.42	0.21	1.15	31.7%		
C × G	2	1.33	0.66	3.65	2.7%	*	0.6%
D × F	2	3.53	1.76	9.70	0.0%	**	2.0%
D × G	2	0.02	0.01	0.06	93.8%		
F × G	4	3.10	0.77	4.26	0.2%	**	1.5%
Error	405	73.64	0.18				
(Error)	414	75.23	0.18				50.1%
Total	431	156.44					100.0%

Notes: N = 432, Mean = - 0.13 N, ** = Significant at 1%, * = 5%.

was smaller in the second repetition. This error reduction is reasonable since the experimenter gets more acquainted with the experiment through the repetition.

DISCUSSION

Hereinafter we will set forth the results of the static equilibrium test. The horizontal positioning error of the load point was small (average 0.73 cm) while the vertical one was large (average -3.18 cm). Since the scale of the model was 1/100, these positioning errors equal 0.73 m and -3.18 m, respectively, for a real-scale TRS system with a span of 300 m. Such a large negative error, especially a vertical error, is critical in the carriage of an actual logging cable system. This is because the carriage of such a system must run over the forest canopy with sufficient clearance to avoid damage to the stand.

However, the positioning errors found in this study were not large compared to a related study [3], which reported a scale model test of a single cable with a concentrated load on its midspan. This scale model had a span one meter long with a large sag; the unstretched line length was 1.20 m. The cable used for their scale model was thicker and with a larger modulus of elasticity than those of our model; the cross sectional area and modulus of

elasticity of their model were 1.58 mm² and 100 GPa, respectively. They compared observed coordinates of the concentrated load point on the cable with calculated coordinates obtained from the theory of elastic catenary. The discrepancy between the observed and theoretical coordinates was 0.4% through 0.7% of the span, which is equivalent to 1.2 cm through 2.1 cm in our study's 3 m span model. They mentioned that there was some stiffness in the cable used and that "the elastic effects are insignificant ... owing to the large sag and the relatively inextensible nature of the cable material" [3]. However, they concluded that the error was negligible, or within experimental error.

With regard to the cause of the errors in our scale model test, for the horizontal positioning error, the type of wire rope was the most prominent factor. The thinner the wire rope, the greater the error. The effect is similar in the case of the vertical positioning error of the load. We may interpret this effect and effects of other significant factors in the vertical positioning error of the load as caused by line stretching or loosening of materials. Effects of the maximum line tension and the type of wire rope on the tension error were similar. When the maximum line tension was great and the wire ropes were thin, there was a negative effect on the experiment since stretched lines slacken.

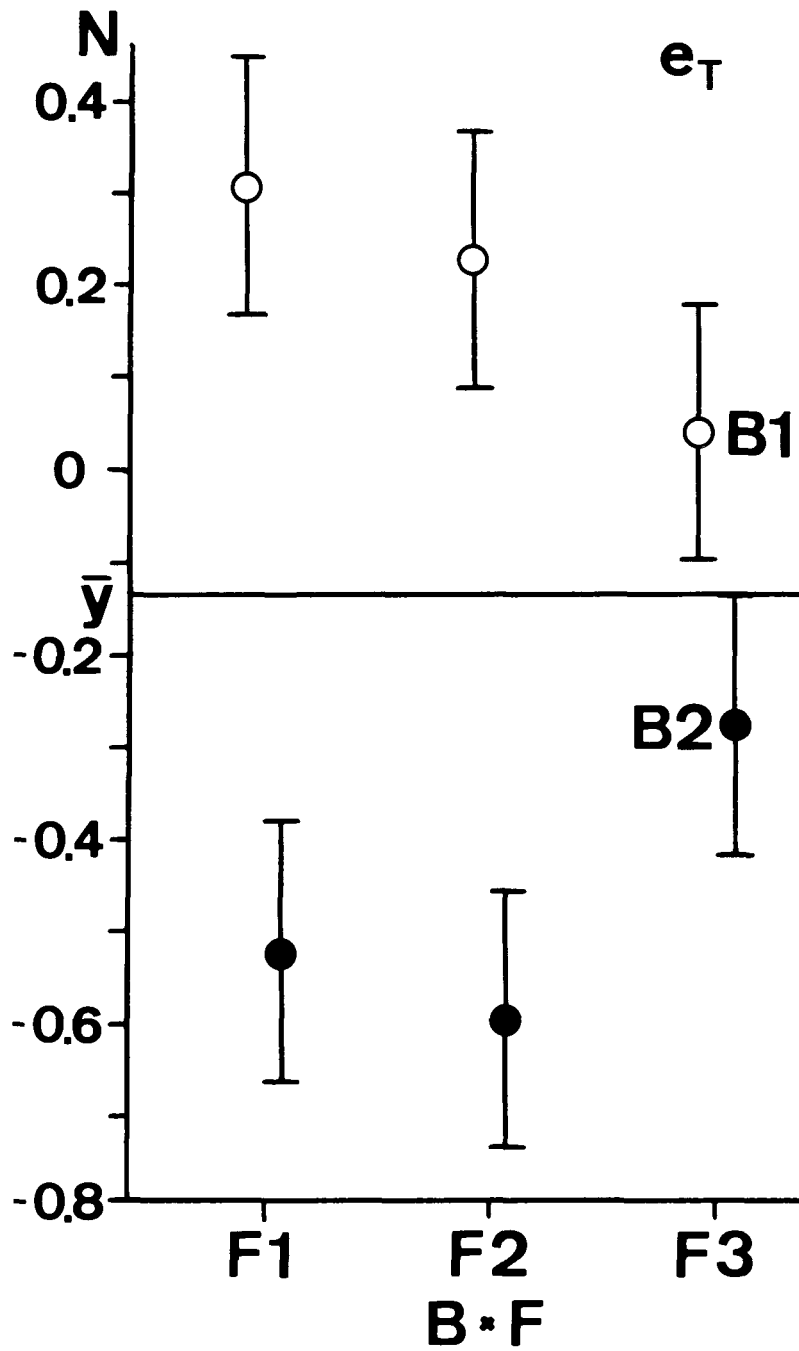


Figure 10. Effects of the maximum line tension (B), the line length (F), and their interaction on e_T , the tension error.

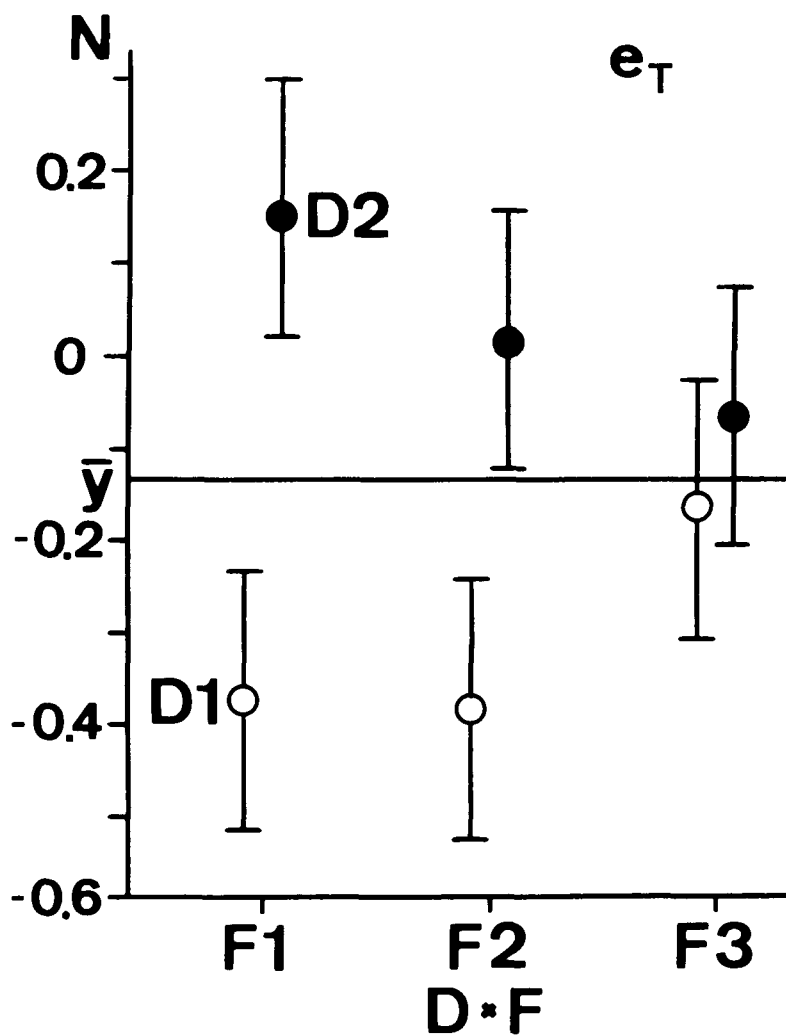


Figure 11. Effects of the type of wire rope (D), the line length (F), and their interaction on e_T , the tension error.

For the anchor point height error, we saw typical responses to the factors relating to experimental error, such as repetition and line number. The effects of line length, which was significant on the anchor point height error, were caused by an inaccurate setting of the theoretical line length. All of these factors were insignificant or had a small r value in positioning and tension errors.

Although the results implied that line stretching could be the main cause of the errors observed, the method that derived theoretical values for the experiment took the effect of line stretching into account. Hence, those errors were possibly caused by overestimation of E , modulus of elasticity of the wire ropes, slipping of lines, and loosening of the framework. However, there can be similar causes in an actual TRS system, that is, bending of spars, loosening and slipping of clips, wear of wire ropes, etc. Therefore, the results of the experiment suggest that in an actual TRS system the horizontal positioning error of the load is small, while the height of the load point might be lower than a designated value. In order to reduce such errors, a more accurate theory should be developed concerning the above-mentioned possible causes. Such an improved theory should be verified via experiments. If the experiment using the improved theory still does not result in good accordance, a practical procedure would have to be developed to reduce the carriage positioning error.

CONCLUSION

In the scale model experiment, the horizontal position of the load point was sufficiently close to the theoretically obtained position, whereas the observed height of the load point was not close to the theoretical value. The carriage tended to be lower in height than the theoretical height. While the positioning error in this study was not large compared to that in a related study [3], effort must be made to reduce the height positioning error of the carriage. A possible recommendation for obtaining a more accurate positioning of the carriage is to take into account additional loosening of lines, guy lines of spars, etc. Furthermore, development of additional theoretical procedures to calculate the configurations of main and slack-pulling lines separately will help to more accurately estimate the carriage position.

NOTE

After this paper was submitted to the *Journal of Forest Engineering*, a theory for separately estimating the configuration of the main and slack pulling lines was developed. A scale model test was conducted to verify this new theory with a scale model having a 10 m span. In this test, movement of the spars was considered. The theory and the results of the test were recently published in *Journal of Forest Research*, Vol. 1, nos. 3 and 4.

ACKNOWLEDGMENTS

We are indebted to Drs. M.G. Gonsior and F.E. Greulich for helpful comments on the manuscript, and to Dr. M.G. Jenkins for advice on the tensile tests. This work was made during a one-year period when the first author studied as a visiting faculty member at the Industrial Engineering Department, University of Washington.

LITERATURE CITED

- [1] Gere, J.M. and S.P. Timoshenko. 1990. *Mechanics of Materials*. 3rd Edition. PWS-KENT. Boston. 807 pp.
- [2] Irvine, H.M. 1981. *Cable Structures*. MIT Press. Cambridge. 259 pp.
- [3] Irvine, H.M. and G.B. Sinclair. 1976. The suspended elastic cable under the action of concentrated vertical loads. *International Journal of Solids Structures* 12: 309-317.
- [4] Kanzaki, K. 1973. On methods of calculations about the three support cable crane supposing static balanced state. *Journal of the Japanese Forestry Society* 55: 173-178. (In Japanese.)
- [5] Kanzaki, K. and T. Sakai. 1972a. Studies on the cable crane hung at three supports (I) (1) A way of calculation supposing static balanced state. *Journal of the Japanese Forestry Society* 54:103-112. (In Japanese with English summary.)
- [6] Kanzaki, K. and T. Sakai. 1972b. Studies on the cable crane hung at three supports (II) (2) Steering problems and possibilities guessed from the computations on static state. *Journal of the Japanese Forestry Society* 54:143-149. (In Japanese with English summary.)

- [7] Kanzaki, K., X. Hong, J. Nishikawa, O. Nishio, and M. Fukutomi. 1986. Studies on cable crane with three supports (triangular running skyline) (VII) Results of selective harvesting operations. *Journal of the Japanese Forestry Society* 68:320-326. (In Japanese with English summary.)
- [8] Mason, R.L., R.F. Gunst, and J.L. Hess. 1989. *Statistical Design and Analysis of Experiments*. John Wiley & Sons, New York. 692 pp.
- [9] O'Brien, T. 1967. General solution of suspended cable problems. *Journal of the Structural Division, ASCE*, 93(ST1):1-26.
- [10] O'Brien, W.T. and A.J. Francis. 1964. Cable movements under two dimensional loads. *Journal of the Structural Division, ASCE*, 90(ST3):89-123.
- [11] Peyrot, A.H. and A.M. Goulois. 1978. Analysis of flexible transmission lines. *Journal of the Structural Division, ASCE* 104(ST5):763-779.
- [12] Peyrot, A.H. and A.M. Goulois. 1979. Analysis of cable structures. *Computers & Structures* 10:805-813.
- [13] Suzuki, Y., E.S. Miyata, and S.C. Iverson. 1996. Static analyses of the triangular running skyline system: a three-dimensionally movable logging cable system. *Computers & Structures*.